Assessment of delocalized and localized molecular orbitals through electron momentum spectroscopy

Assessment of delocalized and localized molecular orbitals through electron momentum spectroscopy*

Liu Yuan(刘 源)[a], Cheung Ling-Fung(张凌峰)[a], and Ning Chuan-Gang(宁传刚)[a)b)†]

[a)] *Department of Physics, State Key Laboratory of Low-Dimensional Quantum Physics, Tsinghua University, Beijing* 100084, *China*
[b)] *Collaborative Innovation Center of Quantum Matter, Beijing, China*

(Received 28 October 2013; revised manuscript received 8 December 2013; published online 10 April 2014)

Recently, there was a hot controversy about the concept of localized orbitals, which was triggered by Grushow's work titled "Is it time to retire the hybrid atomic orbital?" [*J. Chem. Educ.* **88**, 860 (2011)]. To clarify the issue, we assess the delocalized and localized molecular orbitals from an experimental view using electron momentum spectroscopy. The delocalized and localized molecular orbitals based on various theoretical models for CH_4, NH_3, and H_2O are compared with the experimental momentum distributions. Our results show that the delocalized molecular orbitals rather than the localized ones can give a direct interpretation of the experimental (e, 2e) results.

Keywords: electron momentum spectroscopy, delocalized molecular orbital, localized molecular orbital

PACS: 34.80.Gs, 31.15.aj **DOI:** 10.1088/1674-1056/23/6/063403

1. Introduction

The molecular orbital is a powerful and convenient tool for predicting geometric and electronic structures of molecules.[1–4] There are a wealth of different and well-defined types of molecular orbitals in modern quantum chemistry, which are appropriate for different physical processes. Recently, there has been a lot of discussion on the physical meanings of molecular orbitals.[5,6]

The standard *ab initio* calculations, such as the canonical molecular orbital (denoted as HF) of the self-consistent-field (SCF) theory, Kohn–Sham orbital (denoted as KS) of the density functional theory, usually lead to delocalized molecular orbitals (DMO) which generally extend over the entire molecule. The total electron wavefunction of SCF is a single determinant constructed using HF orbitals, which gives a freedom of a unitary transformation without changing the TOTAL electron wavefunction. To relate the *ab initio* quantum chemistry theory to the classic valence bonding concepts, a linear combination of HF orbitals can produce localized molecular orbitals (LMOs) under certain localization procedures. Various localization methods have been proposed, such as the Foster–Boys procedure[7,8] by minimizing the distance between electrons within a molecular; the Pipek–Mezey scheme[9] by maximizing the sum of Mulliken atomic charges; the Edmiston–Ruedenberg approach[10,11] by maximizing repulsion interaction energy of the electrons occupying a molecular orbital; the von Niessen method[12–14] by maximizing the expectation value of the δ function of distance between two electrons (viz. maximizes the self-charge); the natural bond orbitals (NBOs)[15] by maximizing the occupancies in the localized 1- and 2-center regions of the molecule to obtain the elementary Lewis-type dot diagram describing electron orbitals. Natural bond orbitals are widely used for bond analysis. The name is derived from the natural orbitals (NOs) of Löwdin,[16] that are obtained by diagonalizing the one-electron density matrix D. On the NBO basis, the density matrix D is partitioned into blocks $\Gamma^{\sigma\sigma}$, which are related to the highly occupied Lewis-like NBOs, blocks $\Gamma^{\sigma*\sigma*}$ that are related to the low occupancy NBOs such as the anti-bond and the Rydberg bond, and the off-diagonal matrix blocks $\Gamma^{\sigma*\sigma}$, that represent the mixing of high and low occupied orbitals and thus lead to the breakdown of strictly localized Lewis-like orbitals. By using the symmetrized Jacobi rotation, the magnitudes of the off-diagonal elements can be reduced to zero, while the diagonal blocks $\Gamma^{\sigma\sigma}$ and $\Gamma^{\sigma*\sigma*}$ remain unchanged.[17] After this transformation, this new set of orbitals expressed by the NBOs and the Jacobi rotation matrix is called the natural localized molecular orbitals (NLMOs). The so-called "Dyson orbital" is defined by the one-electron ionization process for interpreting the experimental data within the orbital approach. The Dyson orbital and the natural orbital are usually delocalized.

Although the delocalized HF orbital and LMO are equivalent from the view of the TOTAL electron wavefunction, the unitary transformation indeed produces different molecular orbitals. One interesting question is: can we experimentally observe such differences? In the past few decades, several reports have claimed that molecular orbitals were measured using experimental techniques,[18–31] such as the sophisticated femtosecond laser,[18,19] scanning tunneling microscope (STM),[20,21] and electron momentum spectroscopy

*Project supported by the National Natural Science Foundation of China (Grant No. 11174175) and the Tsinghua University Initiative Scientific Research Program, China.

†Corresponding author. E-mail: ningcg@tsinghua.edu.cn

(EMS),[22–24] which have provoked a heated discussion about whether the orbitals can be observed.[32–39] Moreover, recently there was a fierce controversy about the localized orbital,[6,39–46] which was triggered by Grushow's work titled "Is it time to retire the hybrid atomic orbital?".[6] Grushow's idea is challenged by Donald G. Truhlar, who has pointed out that orbitals are theoretical mathematical objects used to construct many-electron wave functions in the form of configuration state.[39] In Schwartz's work titled "Measuring Orbitals: Provocation or Reality",[5] the orbital measurement was defined as the measurement of the one-electron density distribution. The unique feature of EMS is that it can obtain the binding energy and the one-electron density distribution simultaneously for each molecular orbital. In the present work, we try to compare several different types of delocalized and localized orbitals of CH_4, NH_3, and H_2O molecules with experimental EMS results.

2. Theory and experimental methods

The spectrometer used in the present work takes a non-coplanar symmetric (e, 2e) geometry.[24,45,46] The kinetic energies (E_1, E_2) and momenta (p_1, p_2) of two outgoing electrons are determined through the coincidental detection, while the energy (E_0) and momentum (p_0) of the incident electron are pre-defined. The binding energy ε of the bound electron is given by

$$\varepsilon = E_0 - E_1 - E_2. \tag{1}$$

And, the momentum (p) of the bound electron before being knocked out is expressed as[24]

$$p = \left\{ [2p_1\cos\theta - p_0]^2 + \left[2p_1\sin\theta\sin\left(\frac{\phi}{2}\right)\right]^2 \right\}^{1/2}, \tag{2}$$

where θ is the polar angle of the outgoing electrons with respect to the incident electron direction ($\theta_1 = \theta_2 = 45^\circ$), and ϕ is the relative azimuthal angle between the two outgoing electrons.

Under high impact energy and large momentum transfer, the differential (e, 2e) cross section can be factorized into the product of a structural factor and a kinematic term, while the later term is approximately constant. Therefore, the differential cross section of (e, 2e) under a plane wave impulsive approximation (PWIA) can be written as[24]

$$\sigma_{\mathrm{EMS}} \propto S_{\mathrm{i}}^{\mathrm{f}} \int \mathrm{d}\Omega \left| \left\langle \mathrm{e}^{-\mathrm{i}pr} \Psi_{\mathrm{f}}^{N-1} | \Psi_{\mathrm{i}}^{N} \right\rangle \right|^2, \tag{3}$$

where $S_{\mathrm{i}}^{\mathrm{f}}$ represents the spectroscopic factor, $\mathrm{e}^{-\mathrm{i}pr}$ denotes the plane wave, Ψ_{i}^{N} and Ψ_{f}^{N-1} are the wave functions of the ground state and the ionized state of the target, respectively, N is the total electron number, $\int \mathrm{d}\Omega$ represents the spherical average for the randomly oriented molecules in gas phase. The overlap integral $\langle \Psi_{\mathrm{f}}^{N-1} | \Psi_{\mathrm{i}}^{N} \rangle$ is called Dyson orbital,[24,47–50] which can be calculated using the many-body theories, such as the configure interaction, or Green's function theory. In this sense, Dyson orbital is determined by the ionization process. The calculated Dyson orbital is usually expressed as a linear combination of Hartree–Fock orbitals. If Ψ_{f}^{N-1} and Ψ_{i}^{N} are single determinants, under the frozen orbital approximation, equation (3) can be simplified into

$$\sigma_{\mathrm{EMS}} \propto S_{\mathrm{i}}^{\mathrm{f}} \int \mathrm{d}\Omega \left| \varphi_j(p) \right|^2, \tag{4}$$

where $\varphi_j(p)$ is the j-th molecular orbital in the momentum space, which can be a Hartree–Fock orbital[21] or a Kohn–Sham orbital.[51,52] See the appendix for details of the derivation.

In the present work the Dyson orbitals are generated using the symmetry-adapted-cluster configuration-interaction (SAC-CI) theory, which was originally developed by Hiroshi Nakatsuji.[53] The SAC-CI can calculate singlet, doublet, and up to septet state of molecules. The SAC-CI theory has been used to explain the (e, 2e) binding energy spectra of furan, pyrrole, and thiophene,[54] CS_2,[55] and CO_2.[56] Recently, we have introduced the SAC-CI method to calculate the momentum distributions of Dyson orbitals.[57–59] A home-compiled program, NEMS, is used to calculate the spherically averaged momentum distributions of Dyson orbitals.[60] The theoretical momentum distributions of HF orbital, KS orbital, NO, NBO, and NLMO are also generated for comparison. The widely used B3LYP (Becke-3-parameter-Lee–Yang–Parr) hybrid exchange–correlation functional[61,62] is employed in the density functional theory (DFT) calculation. In all of our calculations the Aug-cc-pVTZ basis set is used.[63–65]

The measurement is conducted on our 3rd generation high resolution spectrometer.[45] The energy resolution is 0.7 eV (full width at half maximum, FWHM). The polar angle θ for acceptance is $\pm 0.53^\circ$, and the resolution for azimuthal angle ϕ is $\pm 0.84^\circ$.

3. Results and discussion

Figure 1 shows the experimental (e, 2e) results of CH_4 molecule. Figure 1(a) is the energy–momentum density distribution map measured at the electron impact energy 1200 eV. There are three features in the map. The feature at 14.2 eV, which is related to the $1t_2$ molecular orbital, has a minimum intensity at the azimuthal angle $\phi = 0^\circ$ and a maximum intensity at $\phi = 7^\circ$. In contrast, the feature at 23.2 eV, which is related to the $2a_1$ molecular orbital, has a maximum intensity at $\phi = 0^\circ$. The feature at around 32 eV is mainly composed of satellites of $2a_1$, which is the result of many-body effects. Figure 1(b) is the experimental binding energy spectrum by summing over the observed intensities of all azimuthal angle ϕ. The two main peaks are the results of the ionization from

$1t_2$, $2a_1$ orbitals, respectively. Figure 1(c) presents the spherically averaged experimental momentum distributions of $1t_2$ and $2a_1$, which are obtained from Fig. 1(a) by plotting the intensity of each peak against the azimuthal angle ϕ (converted to momentum p using Eq. (2)). In Fig. 1(c), the experimental momentum distributions are compared with the theoretical ones generated using various models. It can be seen that the predictions using delocalized Dyson, HF, and KS orbitals are in excellent agreement with the experimental distributions, while the predictions of localized NBO and NLMO distributions are remarkably different from the experimental results. As shown in Fig. 1(d), according to NBO or NLMO analysis, the valence orbitals of CH_4 include four equivalent lobes, and each is localized at one CH bond. This picture is consistent with the hybrid valence bond theory. To explain why CH_4 has a tetrahedral structure, the valence bond theory says that two 2s electrons and two 2p electrons of the carbon atom of CH_4 rearrange themselves in a process called hybridization. This reorganizes the electrons into four identical hybrid orbitals, which are called sp^3 hybrids. The sp^3 hybrid orbitals are oriented at a bond angle of 109.5° with respect to each other. This 109.5° arrangement gives rise to tetrahedral geometry. However, as shown in Fig. 1(c), the theoretical momentum distributions using NBO or NLMO cannot explain why $1t_2$ and $2a_1$ orbitals have quite different experimental distributions. They significantly overestimate the intensity in the low momentum region for $1t_2$ orbital, and underestimate the intensity in the low momentum region for $2a_1$. The NOs look the same as HF orbitals, which is due to the triple degeneracy of $1t_2$ orbital. NOs are usually different from HF orbitals (see the figures later on).

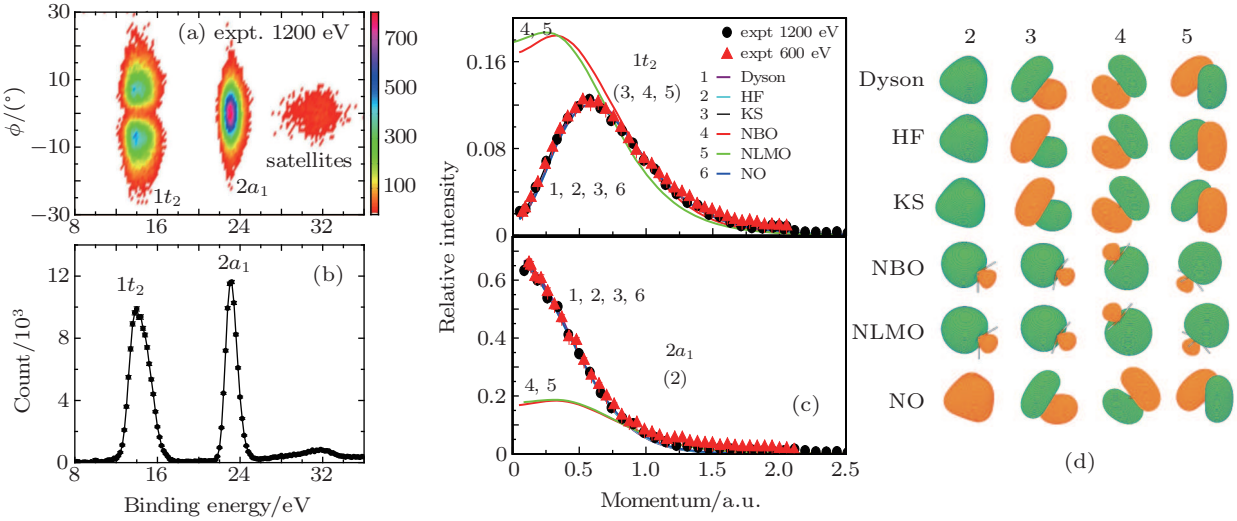

Fig. 1. (color online) Electron momentum spectroscopy of CH_4, showing (a) the energy–momentum density map measured at the electron impact energy 1200 eV, (b) the experimental binding energy spectrum by summing over the observed intensities of all values of azimuthal angle ϕ, (c) the spherically averaged experimental momentum distributions at the electron impact energies 1200 eV and 600 eV for $1t_2$ and $2a_1$ molecular orbitals in comparison with the various theoretical distributions, with the numbers in the parentheses denoting the orbital orders, (d) the molecular orbitals plotted at a contour value 0.04 using different theoretical models, with the numbers on the top referring to the molecular orbital orders, and HOMO ($1t_2$) being the fifth molecular orbital,

It should be noted that there is no one-to-one correspondence between delocalized molecular orbitals and localized molecular orbitals. In Fig. 1(d), Dyson, HF, and KS are ordered according to the magnitudes of their ionization energies. SAC-CI theory predicts that the ionization energies of Dyson orbitals $1t_2$ and $2a_1$ are 14.0 eV and 22.8 eV respectively, which are close to the experimental values 14.2 eV and 23.2 eV. With Koopmans's theorem, the ionization energies of $1t_2$ and $2a_1$ are 14.8 eV, and 25.7 eV respectively, which are the negative values of the HF orbital energies. Since the electron correlation is not taken into account, HF predictions are usually too high. There is a generalized Koopmans's theorem for density functional theory (DFT).[66] With B3LYP functional, the ionization energies of $1t_2$ KS orbital and $2a_1$ orbital are 10.8 eV, and 19.0 eV, respectively. The DFT predictions are usually too low due to the asymptotic error.[67] However, there was no ionization energy directly related to an NBO, NLMO, or NO, so they are simply reordered according to the HF orbital that they look most like.

Figure 2 shows the electron momentum spectroscopy of NH_3. It can be seen that the calculated distributions based on the delocalized Dyson, HF, KS orbitals accord very well with the experimental distributions of $3a_1$, $1e$, and $2a_1$ orbitals. The $3a_1$ and doubly degenerated $1e$ orbitals look like an atomic p-type orbital, and have almost zero intensity at momentum $p = 0$. The $2a_1$ looks like an atomic s-type orbital. It has a maximum intensity at momentum $p = 0$. The calculated electron momentum distributions based on NBOs, NLMOs, and

NOs cannot describe the experimental observations. As shown in Fig. 2(b), according to the NBO theory the four paired valence electrons of NH_3 are arranged as one lone pair that are localized at the nitrogen atom, and three equivalent hybridized pairs located at each NH bond.

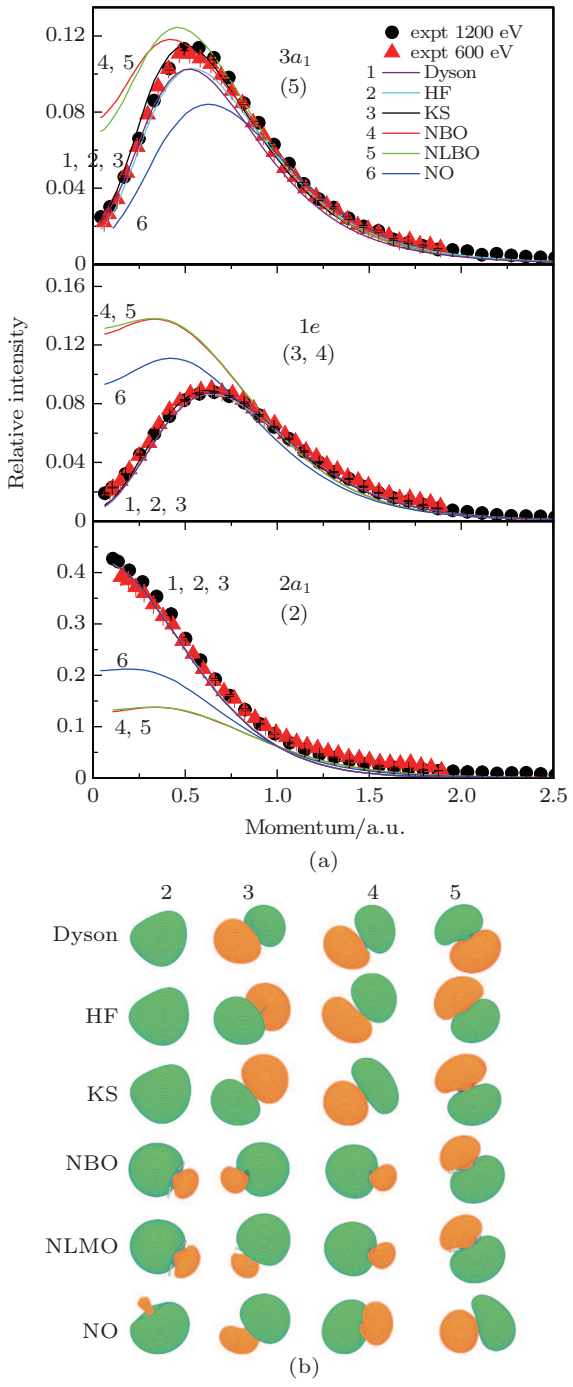

Fig. 2. (color online) Electron momentum spectroscopy of NH_3, showing (a) the spherically averaged experimental momentum distributions at the electron impact energies 1200 eV and 600 eV for $3a_1$, $1e$, and $2a_1$ molecular orbitals in comparison with the various theoretical distributions, with the numbers in the parentheses denoting the orbital orders, and (b) molecular orbitals plotted at a contour value 0.04 using different theoretical models, with the numbers on the top referring to the molecular orbital orders, and HOMO ($3a_1$) being the fifth molecular orbital.

Figure 3 shows the electron momentum spectroscopy of H_2O. The experimental electron momentum distributions are cited from our previous study.[68] Again, the calculated distributions based on the delocalized Dyson, HF, KS orbitals accord well with the experimental distributions of $1b_1$, $3a_1$, $1b_2$, and $2a_1$ orbitals. The $1b_1$, $3a_1$, and $1b_2$ orbitals are of p-type, each having a nodal plane, and almost zero intensity at momentum $p = 0$. The $2a_1$ looks like an atomic s-type orbital, which has a maximum intensity at momentum $p = 0$. The highest occupied molecular orbitals (HOMOs) predicted by Dyson, HF, KS, NBO, NLMO, and NO are very similar. They all well describe the experimental distributions of $1b_1$. However, the calculated electron momentum distributions based on NBOs, NLMOs, and NOs cannot describe the experimental distributions of $3a_1$, $1b_2$, and $2a_1$ orbitals.

From the above comparisons of these molecular orbital models with the experimental distributions, it is safe to conclude that delocalized molecular orbitals are better models than LMOs to describe the experimental results of (e, 2e). The equivalence between delocalized HF orbitals and LMOs is only true for the TOTAL electron wavefunction (a Slater determinant) and it is not true for the one-electron wavefunction. Although a unitary transformation will not change the value of the Slater determinant, it will change the occupation of electrons when considering that electrons actually occupying the different energy levels. Since an electron is a fermion, as a consequence of the Pauli principle only one fermion can occupy a particular quantum state at any given time. An HF orbital is an eigenstate of the Fock operator, but a linear combination of HF orbitals related to different energy levels is no longer an eigenstate. With Koopmans's theorem,[69] the negative value of an HF orbital energy is roughly equal to the ionization energy, and HF orbital approximates to Dyson orbital. There is a similar theorem for KS orbital.[52] The delocalized HF orbital and KS orbital can be directly or approximately measured through experimental techniques, such as (e, 2e), STM, or a femtosecond laser.

Of course, it should be noted that both delocalized and localized orbitals are theoretical mathematical objects that are used to construct many-electron wave functions in the form of configurations.[39] To accurately describe the electron distributions, one may need more than one configuration. Nevertheless, in many cases, the many-electron wave functions can be well approximated using a single configuration if the electron correlation is not strong. The single configuration is written in a form of a Slater determinant, which is an antisymmetrized product of spin orbitals. Since a unitary transformation of a determinant does not change the value of the Slater determinant, there is more than one set of orbitals. "Two sets of orbitals have been found to be of particular significance.

The first set, called molecular orbitals, each has a symmetry that is determined by the nuclear framework and generally spreads throughout the molecule. If an electron is removed from a molecule, it should be regarded as removed from a molecular orbital. The other set of orbitals, called equivalent orbitals, give rise to more localized descriptions of charge corresponding to the various bonds or lone pairs of the molecule."[70] The delocalized orbital is the right choice for the independent-particle picture. Once the process involves excitation, ionization, detachment, or charge-transfer, only the delocalized molecular orbital can provide a simple and concise explanation.[5] In other words, the localized molecular orbital is the right language for the discussion of the chemical bonds, molecular geometric structure, and electrostatic effects. Localized molecular orbitals are equivalent to delocalized HF orbitals that describe the TOTAL electron wavefunction, but the localized molecular orbital is not a right wavefunction describing an independent particle.

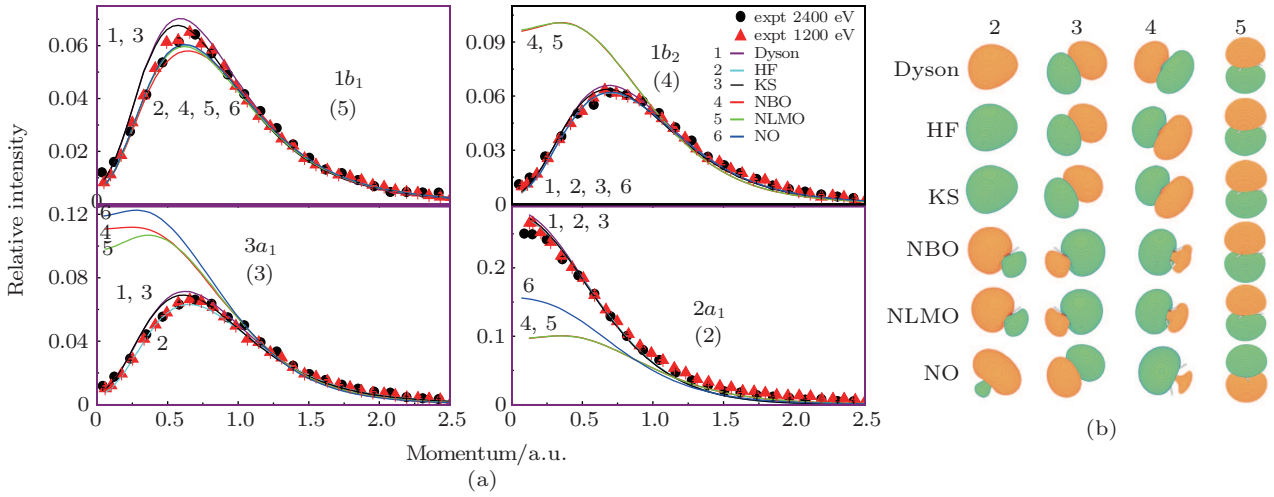

Fig. 3. (color online) Electron momentum spectroscopy of H_2O showing (a) the spherically averaged experimental momentum distributions at the electron impact energies 1200 eV and 600 eV for $1b_1$, $3a_1$, $1b_2$, and $2a_1$ molecular orbitals in comparison with the various theoretical calculations, the numbers in the parentheses denoting the orbital orders, and (b) molecular orbitals plotted at a contour value 0.04 using different theoretical models, the labels on the top referring to the molecular orbital orders, and HOMO ($1b_1$) is the fifth molecular orbital.

4. Conclusions

Experimental one-electron momentum distributions of CH_4, NH_3, H_2O are compared with the theoretical one-electron momentum distributions calculated using various delocalized and localized molecular orbital models. The theoretical momentum distributions based on the delocalized Dyson, HF, and KS orbitals are in excellent agreement with the experimental results. In contrast, the predicted one-electron momentum distributions based on the localized NBO, NLMO, and NO are overall wrong. The delocalized Dyson, HF, and KS orbitals can provide a simple and concise explanation for the ionization potentials and the momentum distributions measured using (e, 2e) spectroscopy, but they cannot provide a simple and concise explanation for localized molecular orbitals. Although LMOs and delocalized HF orbitals are equivalent when describing the TOTAL electron wavefunction, they have different usages. The delocalized HF or KS orbital is a wavefunction of an independent particle, and is a right choice for interpreting the ionization process, but LMO is not. LMO is a correct language for discussing chemical bonds, molecular geometric structure, and electrostatic effects. Of course, it should be noted that LMO has new applications in modern quantum chemistry. LMOs are more frequently used as reference orbitals for speeding up high-level electronic structure calculations by taking advantage of the local nature of electron correlations.

Appendix A

In a more accurate form, the Dyson ϕ^{d} orbital is written as

$$\phi^{\mathrm{d}} = \sqrt{N}\langle \Psi_{\mathrm{F}}^{N-1} | \Psi_{\mathrm{I}}^{N} \rangle. \tag{A1}$$

The bracket integral runs over the space of $N-1$ electrons. The initial Ψ_{I}^{N} and the final Ψ_{F}^{N-1} are Slater determinant type of total wave functions of molecular system.

$$\Psi_{\mathrm{I}}^{N} = \frac{1}{\sqrt{N!}} \begin{vmatrix} \phi_1(1) & \phi_1(2) & \dots & \phi_1(N) \\ \phi_2(1) & \phi_2(2) & \dots & \phi_2(N) \\ \dots & \dots & \dots & \dots \\ \phi_N(1) & \phi_N(2) & \dots & \phi_N(N) \end{vmatrix}, \tag{A2}$$

where ϕ_i is the orthonormal molecular orbital. Supposing that the j-th electron in the s-th initial molecular orbital is ionized, in the frozen orbital approximation, we have

$$\Psi_{\mathrm{F}}^{N-1}=\frac{1}{\sqrt{(N-1)!}}\begin{vmatrix}\phi_1(1) & \phi_1(2) & \cdots & \phi_1(j-1) & \phi_1(j+1) & \cdots & \phi_1(N)\\ \phi_2(1) & \phi_2(2) & \cdots & \phi_2(j-1) & \phi_2(j+1) & \cdots & \phi_2(N)\\ \cdots & \cdots & \cdots & \cdots & \cdots & \cdots & \cdots\\ \phi_{s-1}(1) & \phi_{s-1}(2) & \cdots & \phi_{s-1}(j-1) & \phi_{s-1}(j+1) & \cdots & \phi_{s-1}(N)\\ \phi_{s+1}(1) & \phi_{s+1}(2) & \cdots & \phi_{s+1}(j-1) & \phi_{s+1}(j+1) & \cdots & \phi_{s+1}(N)\\ \cdots & \cdots & \cdots & \cdots & \cdots & \cdots & \cdots\\ \phi_N(1) & \phi_N(2) & \cdots & \phi_N(j-1) & \phi_N(j+1) & \cdots & \phi_N(N)\end{vmatrix}. \tag{A3}$$

The upper $(N-1)\times(N-1)$ determinant is the minor of the determinant of Eq. (A2) by eliminating the s-th row and j-th column, noted as $M_{s,j}$. Now we calculate expression (A1) using expressions (A2) and (A3). Since expression (A2) is an $N\times N$ determinant and expression (A3) is an $(N-1)\times(N-1)$ determinant, we expand expression (A2) by its s-th row and then, we can obtain N determinants whose sizes are $(N-1)\times(N-1)$. The i-th term is $(-1)^{s+i}\phi_s(i)M_{s,i}$. $M_{s,i}$ is the minor of the determinant of expression (A2) by eliminating the s-th row and the i-th column. Therefore,

$$\phi^{\mathrm{d}}=\sqrt{N}\left\langle\Psi_{\mathrm{F}}^{N-1}|\Psi_{\mathrm{I}}^{N}\right\rangle=\sqrt{N}\int\sum_{i}^{N}(-1)^{s+i}\phi_s(i)M_{s,i}\times\frac{1}{\sqrt{N!}\sqrt{(N-1)!}}M_{s,j}^{*}\mathrm{d}r_1\cdots\mathrm{d}r_{j-1}\mathrm{d}r_{j+1}\cdots\mathrm{d}r_N. \tag{A4}$$

Since $\{\phi_i\}$ are orthonormal between each other, $\left\langle M_{s,j}|M_{s,i}\right\rangle$ is nonzero only when $i=j$. We have

$$\begin{aligned}\phi^{\mathrm{d}}&=(-1)^{s+i}\phi_s(j)\frac{\sqrt{N}}{\sqrt{N!}\sqrt{(N-1)!}}\\&\quad\times\int M_{s,j}M_{s,j}^{*}\mathrm{d}r_1\cdots\mathrm{d}r_{j-1}\mathrm{d}r_{j+1}\cdots\mathrm{d}r_N\\&=(-1)^{s+i}\phi_s(j).\end{aligned} \tag{A5}$$

Note that $\int M_{s,j}M_{s,j}^{*}\mathrm{d}r_1\cdots\mathrm{d}r_{j-1}\mathrm{d}r_{j+1}\cdots\mathrm{d}r_N=(N-1)!$ because $\{\phi_i\}$ is an orthonormal set. Thus we have

$$\left|\phi^{\mathrm{d}}\right|^2=|\phi_s(j)|^2. \tag{A6}$$

Why do the NO, NBO, and NLMO deviate from the (e, 2e) experimental results? A further explanation will be given below. Within the framework of the independent particle model, the HF and KS orbitals are the real wave functions of a single electron. The final ionized state can be written in the form of expression (A3) in the frozen orbital approximation. Obviously, the derivation of expression (A6) requires two conditions: the frozen orbital approximation and $\{\phi_i\}$ are in an orthonormal set. The NO, NBO, and NLMO orbitals are orthonormal, but they are not real wave functions of a single electron. No frozen orbital approximation holds for NO, NBO, and NLMO orbitals! We cannot say ionizing the j-th electron from the s-th NO, NBO, or NLMO orbital because they are not the eigenstate of an independent particle. Since NO, NBO, NLMO are the linear combination of HF orbitals, the ionized electron is not from any one NO, NBO, or NLMO, but from many parts of NOs, NBOs, or NLMOs. This is the reason why NO, NBO, and NLMO cannot be directly used to explain processes relating to ionization. The NO, NBO, or NLMO orbitals are equivalent to HF orbitals only for constructing the TOTAL molecular wavefunction. NO, NBO, and NLMO are not the wavefunction of an independent particle, but HF and KS orbitals are a real wavefunction of an independent particle. This is where the problem lies.

References

[1] Mulliken R S 1927 *Phys. Rev.* **29** 637
[2] Mulliken R S 1928 *Phys. Rev.* **32** 186
[3] Mulliken R S 1955 *J. Chem. Phys.* **23** 1833
[4] Mulliken R S 1967 *Science* **157** 13
[5] Schwarz W H E 2006 *Angew. Chem. Int. Ed.* **45** 1508
[6] Grushow A 2011 *J. Chem. Educ.* **88** 860
[7] Boys S F 1960 *Rev. Mod. Phys.* **32** 296
[8] Foster J M and Boys S F 1960 *Rev. Mod. Phys.* **32** 300
[9] Pipek J and Mezey P G 1989 *J. Chem. Phys.* **90** 4916
[10] Edmiston C and Ruedenberg K 1963 *Rev. Mod. Phys.* **35** 457
[11] Edmiston C and Ruedenberg K 1965 *J. Chem. Phys.* **43** s97
[12] von Niessen W 1972 *J. Chem. Phys.* **56** 4290
[13] von Niessen W 1972 *Theor. Chim. Acta* **27** 9
[14] von Niessen W 1973 *Theor. Chim. Acta* **29** 29
[15] Foster J P and Weinhold F 1980 *J. Am. Chem. Soc.* **102** 7211
[16] Löwdin P O 1955 *Phys. Rev.* **97** 1474
[17] Reed A E and Weinhold F 1985 *J. Chem. Phys.* **83** 1736
[18] Zewail A H 2001 *Nature* **412** 279
[19] Zewail A H 2000 *Angew. Chem.* **112** 2688
[20] Lu X H, Grobis M, Khoo K H, Louie S G and Crommie M F 2003 *Phys. Rev. Lett.* **90** 096802
[21] Biedermann A, Genser O, Hebenstreit W, Schmid M, Redinger J, Podloucky R and Varga P 1996 *Phys. Rev. Lett.* **76** 4179
[22] Coplan M A, Moore J H and Doering J P 1994 *Rev. Mod. Phys.* **66** 985
[23] Brion C E 1986 *Int. J. Quantum Chem.* **29** 1397
[24] Weigold E and McCarthy I E 1999 *Electron Momentum Spectroscopy* (New York: Kulwer Academic) pp. 1–129
[25] Liu K, Deng J K and Ning C G 2010 *Chin. Phys. Lett.* **27** 073403
[26] Li W B, Zhu L F, Liu X J, Yuan Z S, Sun J M, Cheng H D and Xu K Z 2004 *Chin. Phys. Lett.* **21** 656
[27] Fan X W, Liao T H, Zhang X Z, Gao J H, Wei J Y and Leung K T 2004 *Chin. Phys. Lett.* **21** 478
[28] Xu R Q, Zhang W H and Li J M 2002 *Chin. Phys. Lett.* **19** 1085
[29] Yang Y, Ji Z H, Yuan J P, Wang L R, Zhao Y T, Ma J, Xiao L T and Jia S T 2012 *Acta Phys. Sin.* **61** 213301 (in Chinese)
[30] Shi L L, Liu K, Luo Z H and Ning C G 2011 *Chin. Phys. B* **20** 113403
[31] Chen J X and Gong Q H 2005 *Chin. Phys.* **14** 1960
[32] Scerri E R 2000 *J. Chem. Educ.* **77** 1492
[33] Spence J C H, Keeffe M O and Zuo J M 2001 *J. Chem. Educ.* **78** 877
[34] Labarca M and Lombardi O 2010 *Found. Chem.* **12** 149
[35] Scerri E R 2001 *Philos. Sci.* **68** 76
[36] Scerri E R 2002 *J. Chem. Educ.* **79** 210
[37] Ostrovsky V N 2005 *Hyle: International Journal for Philosophy of Chemistry* **11** 101
[38] Mulder P 2011 *Hyle: International Journal for Philosophy of Chemistry* **17** 24
[39] Truhlar D G 2012 *J. Chem. Educ.* **89** 573
[40] DeKock R L and Strikwerda J R 2012 *J. Chem. Educ.* **89** 569

[41] Tro N J 2012 *J. Chem. Educ.* **89** 567
[42] Grushow A 2012 *J. Chem. Educ.* **89** 578
[43] Hiberty P C, Volatron F and Shaik S 2012 *J. Chem. Educ.* **89** 575
[44] Landis C R and Weinhold F 2012 *J. Chem. Educ.* **89** 570
[45] Ning C G, Zhang S F, Deng J K, Liu K, Huang Y R and Luo Z H 2008 *Chin. Phys. B* **17** 1729
[46] Ren X G, Ning C G, Deng J K, Zhang S F, Su G L, Huang F and Li G Q 2005 *Rev. Sci. Instrum.* **76** 063103
[47] Singh R K, Ortiz J V and Mishra M K 2010 *Int. J. Quantum. Chem.* **110** 1901
[48] Yamazaki M, Horio T, Kishimoto N and Ohno K 2007 *Phys. Rev. A* **75** 032721
[49] Casida M E and Chong D P 1991 *Int. J. Quantum Chem.* **40** 225
[50] Oana C M and Krylov A I 2007 *J. Chem. Phys.* **127** 234106
[51] Kohn W and Sham L J 1965 *Phys. Rev.* **140** A1133
[52] Duffy P, Chong D P, Casida M E and Salahub D R 1994 *Phys. Rev. A* **50** 4707
[53] Nakatsuji H 1978 *Chem. Phys. Lett.* **59** 362
[54] Ehara M, Ohtsuka Y, Nakatsuji H, Takahashi M and Udagawa Y 2005 *J. Chem. Phys.* **122** 234319
[55] Huang C W, Shan X, Zhang Z, Wang E, Li Z and Chen X J 2010 *J. Chem. Phys.* **133** 124303
[56] Tian Q G, Shi J Y, Shi Y F, Shan X and Chen X J 2012 *J. Chem. Phys.* **136** 094306
[57] Miao Y R, Ning C G, Liu K and Deng J K 2011 *J. Chem. Phys.* **134** 204304
[58] Miao Y R, Deng J K and Ning C G 2012 *J. Chem. Phys.* **136** 124302
[59] Miao Y R, Ning C G and Deng J K 2011 *Phys. Rev. A* **83** 062706
[60] Ning C G, Ren X G, Deng J K, Su G L, Zhang Z F, Knippenberg S and Deleuze M S 2006 *Chem. Phys. Lett.* **421** 52
[61] Becke A D 1993 *J. Chem. Phys.* **98** 5648
[62] Lee C, Yang W and Parr R G 1988 *Phys. Rev. B* **37** 785
[63] Kendall R A, Dunning T H and Harrison R J 1992 *J. Chem. Phys.* **96** 6796
[64] Woon D E and Dunning T H 1993 *J. Chem. Phys.* **98** 1358
[65] Dunning T H 1989 *J. Chem. Phys.* **90** 1007
[66] Dabo I, Ferretti A, Poilvert N, Li Y L, Marzari N and Cococcioni M 2010 *Phys. Rev. B* **82** 115121
[67] Baer R and Neuhauser D 2005 *Phys. Rev. Lett.* **94** 043002
[68] Ning C G, Hajgato B, Huang Y R, Zhang S F, Liu K, Luo Z H, Knippenberg S, Deng J K and Deleuze M S 2008 *Chem. Phys.* **343** 19
[69] Koopmans T 1934 *Physica* **1** 104
[70] Lennard-Jones J and Pople J A 1951 *Discuss. Faraday Soc.* **10** 9